

A benchmark estimate of the effect of anthropogenic emissions on the ocean surface

Dáithí A. Stone^{1,2,3} and Pardeep Pall^{1,4}

¹Lawrence Berkeley National Laboratory, Berkeley, California, United States of America

²Global Climate Adaptation Partnership, United Kingdom

³National Institute for Water and Atmospheric Research, Wellington, Aotearoa New Zealand

⁴University of Oslo, Oslo, Norway

Abstract

Investigations into the role of anthropogenic emissions in the occurrence of extreme weather often use a method that compares simulations of atmospheric climate models run under a factual scenario of historical boundary conditions observed during the period of the event against simulations run under a counterfactual scenario of what those boundary conditions might naturally have been over that same period in the absence of anthropogenic emissions. A particular requirement for this experiment design is the requirement of an accurate estimation of ocean surface boundary conditions for use by the counterfactual natural simulations. Here we use output from the CMIP5 multi-climate-model archive to develop a robust estimate of sea surface temperatures and sea ice conditions for use in counterfactual natural simulations, intended as a benchmark estimate to facilitate comparison across climate models and across studies. This development includes tests to ensure that the final estimate is stable from year-to-year and stable against other perturbations to the methodology, as well as consideration of the strengths and weaknesses in comparison to other available attributable warming estimates. While this estimate is tailored specifically for the International CLIVAR C20C+ Detection and Attribution Project, it can be used by related projects as well.

1 Introduction

Growing interest in the role of anthropogenic emissions in recent and current extreme weather (labeled “event attribution” in this paper) has been reflected in a rapidly growing number of studies (e.g. see summaries in Stott et al. 2013; Bindoff et al. 2013; National Academies of Sciences, Engineering, and Medicine 2016; Herring et al. 2018). One of the more popular methods for evaluating the role of emissions in observed climate change involves the comparison of climate model simulations run under a “real-world” factual scenario against simulations of the same climate model run under a “natural-world” counterfactual scenario of what the world might have been in the absence of anthropogenic emissions (Gillett et al. 2016). More specifically, simulations in the factual scenario are run under observed historical boundary conditions, including variations in anthropogenic and natural factors such as greenhouse gas concentrations, aerosol burdens (or emissions), ozone concentrations, stratospheric volcanic aerosol burden, solar insolation, and land cover and use. The counterfactual simulations are run under the same natural boundary conditions (volcanic aerosols and solar insolation), but with the anthropogenic drivers set

33 at preindustrial values. The large sample size required for robust statistical characterisa-
34 tion of the properties of extreme (and hence rare) weather is provided by running multiple
35 simulations under each scenario, with each simulation beginning from a different initial
36 state. A comparison between the two sets of simulations of the frequency of exceedance
37 of a threshold or some other property of the extremes hence provides a measure of the
38 anthropogenic role in that event (Stone and Allen 2005).

39 One of the challenges in this climate modelling approach is the need to run a large
40 number of simulations. In addition, models operating at low spatial resolution tend to
41 reproduce the climatology of extreme weather poorly relative to higher resolution models
42 (e.g. Wehner et al. 2014) and also do not always provide useful surrogates for higher
43 resolution models in terms of the anthropogenic response in extreme weather (Wehner
44 et al. 2015). Considering that models of the coupled atmosphere-ocean system also require
45 a large spin-up time from standard initial condition perturbations in order to plausibly
46 satisfy the ergodic assumption, full implementation of this climate modelling approach can
47 be computationally prohibitive. Pall et al. (2011) proposed that computational efficiency
48 could be achieved by running the simulations with an atmosphere (and land)-only model
49 using prescribed ocean surface conditions. This approach not only has the advantage of
50 increased computational efficiency, but also, if simulations are based on observed ocean
51 conditions, of the removal of large biases in the ocean state that can exist in current
52 atmosphere-ocean models.

53 The Pall et al. (2011) approach has a catch, however, in that counterfactual natural-
54 world ocean and sea-ice boundary conditions now have to be produced off-line, and there
55 is no uniquely obvious way for doing so. A number of different approaches have been used,
56 and these will be described in the next section. However, we argue below that in general
57 these estimates are lacking in terms of a number of criteria. While these estimates are
58 plausible and deserving of investigation, it would prove helpful for diagnosing components
59 of uncertainty in event attribution calculations if there were a benchmark estimate that
60 could be used to identify differences in results across atmospheric models and other variable
61 aspects of experiment design. Hence, in this paper we develop a credible benchmark
62 estimate of the natural-world sea surface temperature (SST) and sea ice concentration
63 (SIC) boundary conditions. This is performed by estimating the warming attributing to
64 anthropogenic emissions and then subtracting that estimate from the real-world state.
65 We will refer to the factual real-world state as “All-Hist” (for historical all-forcings), the
66 counterfactual natural-world SSTs (Section 4) and SICs (Section 5) developed here as the
67 “Nat-Hist/CMIP5-est1 SSTs and SICs” (for historical natural-forcings scenario generated
68 using simulations for the CMIP5 archive), and the attributable warming estimate used to
69 calculate the Nat-HIST/CMIP5-est1 SSTs and SICs through subtraction from the All-Hist
70 state as the “Nat-Hist/CMIP5-est1 attributable warming” (Section 4).

71 These Nat-Hist/CMIP5-est1 SSTs and SICs are intended specifically as a benchmark
72 for use by the International CLIVAR C20C+ D&A Project, an international multi-model
73 effort using the atmospheric modelling approach to understand extreme weather in the
74 context of anthropogenic climate change (Stone et al. 2019); in that sense this paper is
75 intended as a traceable account of the experiment design adopted by the project. However,
76 it is hoped that it will also prove useful for other related projects as well. It should also be
77 made clear that this should not be the only SSTs and SICs used for Nat-Hist scenarios; the
78 sensitivity of event attribution conclusions to the estimation of the Nat-Hist ocean found
79 in several studies indicates that it is crucial that multiple estimates be explored (Pall et al.
80 2011; Kay et al. 2011; Christidis et al. 2013; Christidis and Stott 2014; Shiogama et al.
81 2014; Schaller et al. 2016).

2 Constructing counterfactual natural-world surface boundary conditions

The Pall et al. (2011) atmospheric time-slice approach is based on four conditions (Risser et al. 2017):

- The extreme event of interest must occur in the atmosphere (and/or land surface).
- The event, and more specifically the metric comparing the event in the two scenarios, should be at most only weakly dependent on the ocean state, for instance of the occurrence of El Niño events (Risser et al. 2017).
- If the preceding condition is not satisfied, then the aspect of the ocean state on which the event depends, for instance the frequency and anomalous properties of El Niño events, must be unaffected by anthropogenic forcing.
- Short-term coupling between the atmosphere and ocean must not be important for the generation of the event (Trenberth et al. 2015; Dong et al. 2017); this could be an issue for instance for tropical cyclones, which churn up cold water from beneath the mixed layer and thus can undermine the surface conditions conducive to their existence and growth.

While the first condition is fundamental, the other three can also be interpreted as assumptions.

The atmospheric modelling approach has thus converted a modelling issue into an experiment design issue. Along with the forcings described above, such as greenhouse gas concentrations, we now need to prescribe SST and SIC states for both the factual and counterfactual scenario (Table 1). While the specification of the other boundary conditions follows easily from current practice (e.g. Gillett et al. 2016) or from the experiment design, the specification is not so obvious for the ocean and sea ice conditions. In this paper we will assume that the SSTs and SICs for the factual All-Hist simulations are based on observed values. In theory they could also be obtained from simulations of atmosphere-ocean models, but the advantage of using observed values is that it seems most consistent with the experiment design and it removes biases that exist in atmosphere-ocean model outputs. Either way, the exact method for specifying the All-Hist ocean and sea ice state is not important for this paper, which focuses on generation of the counterfactual natural-world SSTs and SICs.

The counterfactual natural-world, hereafter “Nat-Hist” (for historical naturally-forced, of which the Nat-HIST/CMIP5-est1 estimate of SSTs and SICs is one plausible estimate), SSTs and SICs generally must be based on subtraction of a map of attributable change from the All-Hist values. To see why subtraction from the All-Hist values is necessary, consider the situation where observed SSTs and SICs from the 2006-2015 period are used for the All-Hist scenario and the observed values from the approximately pre-industrial 1851-1860 period are used for the Nat-Hist scenario. Suppose that an extreme event actually occurs more frequently under El Niño conditions (so violating the second assumption): then it could matter a great deal whether two El Niño events occurred in one period but only one in the other, or whether the magnitude of the El Niño events differed between the two periods. Because of the small length of these periods relative to the time frame for robust statistical characterisation of El Niño events (possibly centuries), any differences could easily reflect sampling limitations rather than an actual anthropogenic influence on El Niño behaviour. Subtraction of an anthropogenic warming signal from the All-Hist

Table 1: List of time-varying boundary conditions for use in the “All-Hist” and “Nat-Hist” scenarios in the C20C+ D&A project, an international climate modelling effort using the Pall et al. (2011) atmospheric modelling approach to understand past and current extreme weather in the context of anthropogenic climate change. The Nat-Hist/CMIP5-est1 estimate of SSTs and SICs developed in this paper is one estimate of the Nat-Hist scenario. The prescription of land cover/use in Nat-Hist scenarios is not set by the project protocols, and thus depends on whether the relevant modeller considers the interest to be in all anthropogenic forcing or in large-scale forcing.

Forcing	All-Hist	Nat-Hist family
Greenhouse gas concentrations	Historical values	Pre-industrial values
Anthropogenic aerosol burdens or emissions	Historical values	Pre-industrial values
Stratospheric ozone	Historical values	Pre-industrial values
Land cover/use	Historical values	Historical or pre-industrial values
Solar insolation	Historical values	Historical values
Natural aerosol burdens or emissions	Historical values	Historical values
Sea surface temperatures	Historical values	Modified historical values
Sea ice concentrations	Historical values	Modified historical values

127 SSTs, on the other hand, would ensure a like-for-like comparison in terms of the anoma-
 128 lous ocean states. Obviously the accuracy of this approach depends on the assumption
 129 that the effect of emissions on ocean variability is much smaller than sampling uncertainty
 130 arising from several decades of data.

131 Within this paper, we will refer to the quantity being subtracted from the All-Hist
 132 SSTs as the “attributable warming” estimate, it being an estimate of the degree to which
 133 anthropogenic interference with the climate system has warmed the ocean. Note that while
 134 the Nat-Hist/CMIP5-est1 attributable warming estimate is unique, the Nat-Hist/CMIP5-
 135 est1 SSTs and SICs that result from its subtraction from the All-Hist SSTs and SICs can
 136 vary depending on the observational (or other) product used for the All-Hist values.

137 3 Evaluating estimates of attributable warming

138 We propose that there are a number of criteria for a benchmark Nat-Hist attributable
 139 warming estimate and the resulting Nat-Hist SSTs and SICs.

140 **Physical plausibility:** They must be physically plausible. If the attributable warming
 141 estimate is subtracted from observed SSTs and SICs used for the All-Hist scenario,
 142 then at least the variability is physically plausible (assuming anthropogenic forcing
 143 has a minimal effect on ocean variability). So this condition applies more specifically
 144 to the attributable warming estimate.

145 **Robustness:** The Nat-Hist SSTs and SICs must be robust against perturbations to the
 146 method used for estimating the attributable warming signal and against perturba-
 147 tions to the method used to generate SSTs and SICs from that attributable warming
 148 signal.

149 **Obviousness:** A proposed benchmark will be more acceptable as a benchmark only if
 150 users consider it an obvious possible approach. While the above criteria may them-
 151 selves be criteria for the acceptance of a proposed benchmark, here we are referring
 152 to other factors, such as the usage of well-regarded data products and a preference
 153 for simplicity where possible.

154 **Availability:** Files containing the attributable warming estimate and/or the resulting
155 Nat-Hist SSTs and SICs must be publicly downloadable, or code for their calculation
156 must be publicly downloadable.

157 A number of plausible candidates exist already. Estimates based on simulations of
158 a single atmosphere-ocean climate model have been produced and used by a number of
159 studies (Pall et al. 2011; Christidis et al. 2013; Shiogama et al. 2013; Christidis and Stott
160 2014; Wolski et al. 2014; Schaller et al. 2016). These candidates are physically plausible, in
161 that these climate models are explicitly constructed as physically plausible representations
162 of the climate system. The climate model data themselves are readily accessible and the
163 method of calculation is either straightforward or uses readily available code, depending
164 on the details. However, the result is not robust to the selection of climate model (e.g.
165 Pall et al. 2011), and typically available simulations from individual models provide poor
166 sample sizes for accurate estimation of the attributable warming signal. Thus the selection
167 of atmosphere-ocean climate model becomes important, and it is not obvious which one
168 should be selected.

169 An alternative approach is to base the estimate on observed data rather than climate
170 models, using a map of observed linear trends in the historical record (Christidis and Stott
171 2014; Sun et al. 2018). This certainly satisfies the physical plausibility criterion, as the real
172 climate response is embedded in the observed trend (observational errors notwithstanding),
173 even if it is partly hidden by sampling variability. Observed trends also fit the obviousness
174 criterion, as observed trends are a frequent measure used in climate change research, and
175 observed SST and SIC data products are widely available. However, the spatial patterns
176 are not very robust, depending strongly on the interpolation method used to estimate
177 temperatures over large areas of the ocean that were largely unmonitored a century ago
178 (Deser et al. 2010; Hartmann et al. 2013; Kennedy 2014) as well as the specific period of
179 time considered.

180 Bichet et al. (2015) and Bichet et al. (2016) instead used a hybrid observations-climate-
181 model approach, in which simulations of atmosphere-ocean climate models were used to
182 calculate a time-invariant pattern, with the time-varying amplitude of that pattern cal-
183 culated from the observational record. They concluded that the resulting attributable
184 warming estimate reflected about half to three quarters of the actual response to anthro-
185 pogenic forcing, depending on details of the methodology. In contrast to using observed
186 trends, sensitivity to the period used in this pattern scaling approach may mostly reflect
187 the availability of more data when longer periods are used. The method also would seem
188 to satisfy the obviousness criterion. Physical plausibility rests on the assumption that the
189 spatial patterns of forcings which have strong regional characteristics do not change over
190 time, that the sensitivity of the climate system to forcings with different rates of change
191 does not vary across those forcings, and that the response to natural forcings does not
192 project onto the spatial pattern.

193 4 Nat-Hist/CMIP5-est1 attributable warming and SSTs

194 4.1 Data source

195 Our proposed candidate for a benchmark attributable warming estimate follows exist-
196 ing atmosphere-ocean climate model-based approaches, but uses multiple climate models
197 instead of just one. This candidate uses “historical” (representing historical changes in cli-
198 mate driven by both anthropogenic and natural forcings) simulations and “historicalNat”
199 (driven by natural forcings only) simulations from the CMIP5 climate model database

200 (Taylor et al. 2012). These have become the international standard for estimating how we
 201 expect the average climate to have evolved over the past century (historical) and how we
 202 expect it might have evolved in the absence of anthropogenic interference (historicalNat)
 203 (Bindoff et al. 2013), so they can be considered an obvious option. These simulations
 204 have been generated using state-of-the-art coupled atmosphere-ocean models of the cli-
 205 mate system and thus are intended to account for all possible sources of climate variability
 206 on time scales ranging up to the full one and a half centuries covered, thus being explicitly
 207 designed to be physically plausible (although we are invoking an assumption that their
 208 linear average must be physically plausible too). They also provide a much larger sample
 209 size than a single model would, suggesting some robustness. Thus we adopt these simula-
 210 tions for estimation of the Nat-Hist/CMIP5-est1 attributable warming signal by taking the
 211 time-varying difference between the historical and historicalNat simulations (see below).

212 The CMIP5 historical simulations start before the beginning of the 20th century but
 213 end in the year 2005, so we extend them to (and beyond) the present using CMIP5
 214 simulations driven with the RCP4.5 emissions scenario (“rcp45”) which continue on from
 215 the end of the historical simulations; the choice of this scenario is mostly dictated by higher
 216 availability of simulations. No such continuation exists for historicalNat simulations (some
 217 of which end later than 2005) so whenever a historicalNat simulation ends we adopt the
 218 final available year for use in subsequent years; the assumption of constant natural forcings
 219 underlies the RCP4.5 scenario and so this choice ensures that we are still diagnosing
 220 the response to anthropogenic forcing only. Note that application of 5-year temporal
 221 smoothing (explained below) means that values for post-end-of-simulation years in the
 222 final product are in fact informed by the last five available years of simulation.

223 The simulations used are listed in Table 2. Selection is based on:

- 224 • Availability on 1 April 2013.
- 225 • Availability of monthly skin temperature output (see Section 4.3) from simulations
 226 following the historical, rcp45, and historicalNat scenarios.

227 By selecting pairs of historical and historicalNat simulations which share initial condi-
 228 tions, we assume that long-term secular drift is cancelled through the subtraction of the
 229 latter from the former. In total 51 simulations for each scenario (historical&rcp45, his-
 230 toricalNat) from 19 CMIP5 models satisfy these criteria. All data are regridded to the
 231 $1^\circ \times 1^\circ$ longitude-latitude grid of the Hurrell et al. (2008), NOAA OI.v2 (Reynolds et al.
 232 2002), and HadISST1 (Rayner et al. 2003) observational sea surface temperature and sea
 233 ice coverage products, with data retained over ocean as well as over land.

234 4.2 Method

235 In summary, the estimation of the Nat-Hist/CMIP5-est1 attributable warming and SSTs
 236 uses the following steps. Further details are provided in subsequent subsections, but here
 237 we provide a summary for clarity. Let $T(x, m, a, s, h)$ represent the skin temperature and
 238 $SST(x, m, a, s, h)$ represent the sea surface temperature, both at spatial location x during
 239 month m and year a in simulation s run under historical scenario h . A bar over any
 240 independent variable denotes an average across all values, i.e. \bar{m} is the annual average.

- 241 1. We take the monthly mean skin temperature output (see Section 4.3) from the
 242 CMIP5 historical and rcp45 simulations listed in Table 2 for $T(x, m, a, s, historical\&rcp45)$
 243 and CMIP5 historicalNat simulations for $T(x, m, a, s, historicalNat)$.

Table 2: List of CMIP5 “historical”, “rcp45”, and “historicalNat” simulations of atmosphere-ocean models used for estimating the Nat-Hist/CMIP5-est1 attributable warming signal. Simulation labels are those adopted by the CMIP5 data archive and apply to all three scenarios. rcp45 simulations continue from historical simulations with the handover on 1 January 2006, while historicalNat simulations end in different years, depending on the model. A total of 51 simulations from 19 CMIP5 models for each of the scenarios are included in the calculation.

CMIP5 Model	CMIP5 simulation labels	Last year of HistoricalNat simulations
BCC-CSM1-1	r1i1p1	2012
BNU-ESM	r1i1p1	2005
CanESM2	r1i1p1, r2i1p1, r3i1p1, r4i1p1, r5i1p1	2012
CCSM4	r1i1p1, r2i1p1, r4i1p1, r6i1p1	2005
CNRM-CM5	r1i1p1	2012
CSIRO-Mk3-6-0	r1i1p1, r2i1p1, r3i1p1, r4i1p1, r5i1p1	2012
GFDL-CM3	r1i1p1	2005
GFDL-ESM2M	r1i1p1	2005
GISS-E2-H-p1	r1i1p1, r2i1p1, r3i1p1, r4i1p1, r5i1p1	2012
GISS-E2-H-p3	r1i1p3, r2i1p3, r3i1p3, r4i1p3, r5i1p3	2012
GISS-E2-R-p1	r1i1p1, r2i1p1, r3i1p1, r4i1p1, r5i1p1	2012
GISS-E2-R-p3	r1i1p3, r2i1p3, r3i1p3, r4i1p3, r5i1p3	2012
HadGEM2-ES	r1i1p1, r2i1p1, r3i1p1, r4i1p1	2018/2019
IPSL-CM5A-LR	r1i1p1, r2i1p1, r3i1p1	2012
IPSL-CM5A-MR	r1i1p1	2012
MIROC-ESM	r1i1p1	2005
MIROC-ESM-CHEM	r1i1p1	2005
MRI-CGCM3	r1i1p1	2005
NorESM1-M	r1i1p1	2012

- 244 2. We apply a five-year boxcar filter along the year dimension (see Section 4.5), result-
 245 ing in
 246 $T^{5year}(x, m, a, s, h) = \frac{1}{5} \sum_{a'=a-2}^{a+2} T(x, m, a', s, h)$ for $h \in \{historical\&rcp45, historicalNat\}$
- 247 3. For the historicalNat scenario, if the last year a_{last} of a simulation is earlier than
 248 year $a + 2$ (because of the 5-year smoothing above), then we define the value in year
 249 a to be a_{last} :
 250 $T^{5year}(x, m, a, s, h) = T^{5year}(x, m, a_{last}, s, h)$ for $a + 2 > a_{last}$.
- 251 4. We average across all simulations in each scenario, hence
 252 $T^{5year}(x, m, a, \bar{s}, h) = \frac{1}{N_s(h)} \sum_{s=1}^{N_s(h)} T^{5year}(x, m, a, s, h)$
 253 (see Section 4.4). Note that the number of simulations $N_s(h)$ is the same for both
 254 $h \in \{historical\&rcp45, historicalNat\}$ in our implementation.
- 255 5. The Nat-Hist/CMIP5-est1 attributable warming estimate is the difference between
 256 the two scenarios:
 257 $\Delta T^{5year}(x, m, a, \bar{s}, Nat-Hist/CMIP5-est1)$
 258 $= T^{5year}(x, m, a, \bar{s}, historical\&rcp45) - T^{5year}(x, m, a, \bar{s}, historicalNat)$.
- 259 6. The Nat-Hist/CMIP5-est1 SSTs are then calculated by subtracting the Nat-Hist/CMIP5-
 260 est1 attributable warming estimate from the All-Hist (generally observed) SSTs:
 261 $SST(x, m, a, \bar{s}, Nat-Hist/CMIP5-est1)$
 262 $= SST(x, m, a, \bar{s}, All-Hist) - \Delta T^{5year}(x, m, a, \bar{s}, Nat-Hist/CMIP5-est1)$.
 263 Any resulting SSTs that are less than the freezing point (-1.8°C in the observational
 264 products used here for the All-Hist SSTs) are set to the freezing point.

265 In the following subsections, we describe these steps in more detail and examine vari-
 266 ous aspects of the robustness of the Nat-Hist/CMIP5-est1 attributable warming estimate
 267 against decisions made in these steps.

268 4.3 Selection of skin temperature

269 The most obvious temperature measure to use for estimating changes in SSTs might be
 270 SST itself. However, because SST cannot go below the freezing point, it may not accurately
 271 portray changes in surface conditions in the polar regions. Pall et al. (2011) used 1.5m
 272 near-surface temperature partly for this reason. Here though we opt for skin temperature.
 273 It more closely matches SST in the ice-free open ocean, and over ice-covered regions it
 274 reports the temperature at the ice-air interface, and this interface is in fact the surface
 275 boundary as seen by atmospheric models.

276 4.4 Averaging across simulations

277 Either models or simulations could be treated as the basic unit for averaging. When
 278 considering differences between historical&rcp45 and historicalNat simulations over the
 279 recent past and near future, as here, natural autonomous variability of the climate system
 280 accounts for a large fraction of the spread of trends across simulations, which means that
 281 it is a common practice to consider each simulation as equally probable (e.g. Hegerl et al.
 282 2007; Hoegh-Guldberg et al. 2014). Our estimate follows this practice, which also provides
 283 a higher effective sample size that proves useful for reducing sampling noise at small
 284 scales. Taking only one simulation (the “r1ip1” or “r1ip3” simulation for each scenario,
 285 yielding 19 simulations per scenario in total) per model yields a similar difference map
 286 at large scales, but with some regional differences (Figure 1). The rougher appearance

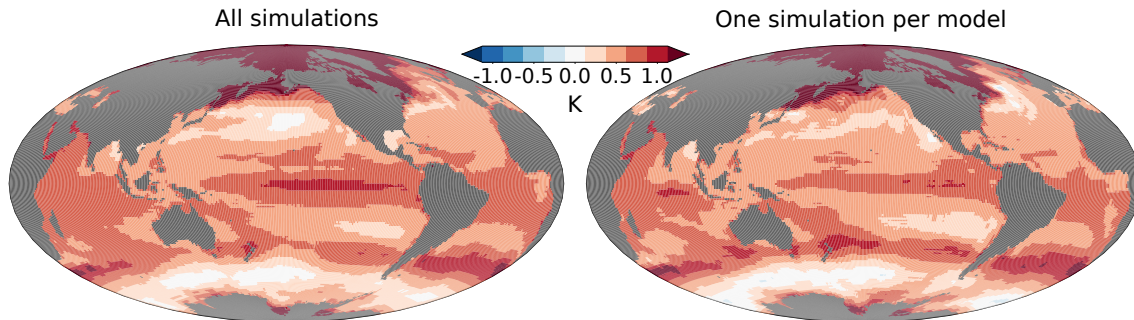


Figure 1: Estimates of the attributable warming for January 2001 using all selected CMIP5 simulations (left) or only one simulation (per scenario) per climate model (right). A 5-year boxcar filter has been used in the year dimension in all calculations (Section 4.5).

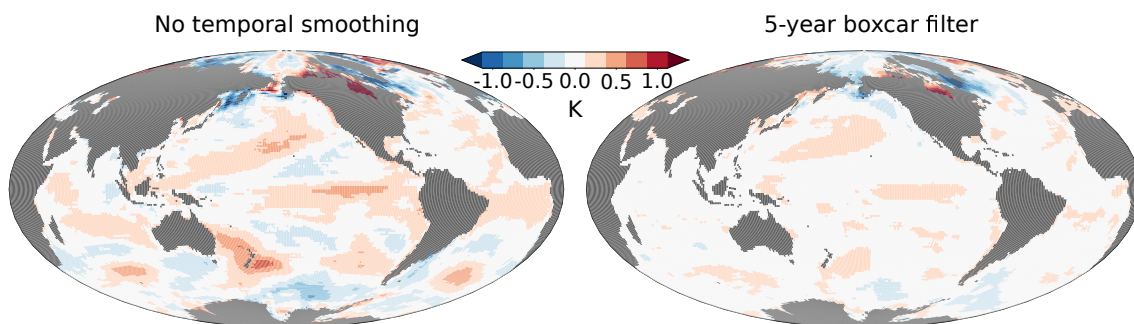


Figure 2: Maps of the difference between January 2006 and January 2001 in estimated attributable warming. The left map is produced without temporal smoothing, while the right map uses a 5-year boxcar filter applied to January data (i.e. the average of the maps from January 2004, 2005, 2006, 2007, and 2008 minus the average for the maps from January 1999, 2000, 2001, 2002, and 2003).

287 of the pattern when only one simulation per model is used suggests that a large part
 288 of this difference is sampling noise in the smaller data set (19 versus 51 simulations per
 289 simulation).

290 4.5 Stability from year to year

291 Despite the use of 51 simulations for each of the historical&rep45 and historicalNat sce-
 292 narios, there may still be noticeable sampling noise at the grid scale of the attributable
 293 warming estimates, which could be important for simulation of regional extreme weather.
 294 Anthropogenic forcing is changing only slightly from year to year, so comparison of nearby
 295 years should reveal little difference if sampling noise is minimal. Figure 2 compares the
 296 attributable warming estimate for January 2006 against the estimate for January 2001
 297 when Step #2 (the 5-year smoothing) is skipped and reveals that, despite use of a large
 298 number of simulations, regional year-to-year variations as large as 0.5°C arise over the
 299 non-polar ocean. One option would be to impose some spatial smoothing (Shiogama et al.
 300 2013), but this could remove local warming gradients that are important for the generation
 301 of extreme weather on and near coasts. Another option is to smooth in time (Shiogama
 302 et al. 2013). Use of a 5-year boxcar filter (note that no overlap occurs for the 2001 and
 303 2006 calculations) applied separately for each calendar month reduces those variations to
 304 about 0.1°C (in ice-free areas) of the global average warming.

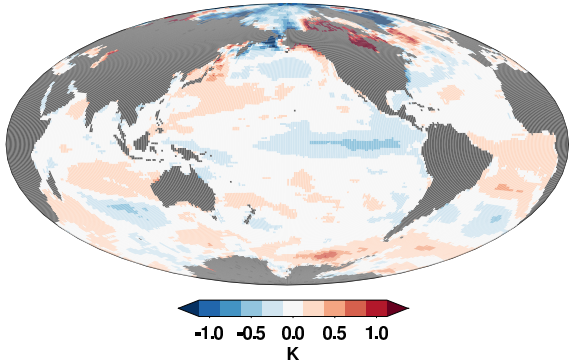


Figure 3: Map of the difference between January 1997 and January 1992 in estimated attributable warming. No temporal filter has been applied in the calculation.

305 One potential issue with a temporal filter is that it smooths out the climate response
 306 to volcanic eruptions. If the sea surface temperature response to a major volcanic eruption
 307 is linearly additive with the response to anthropogenic forcing (Meehl et al. 2003; Gillett
 308 et al. 2004; Shiogama et al. 2012), then the volcanic responses in the historical&rcp45
 309 and historicalNat simulations will cancel, leaving no imprint on the attributable warming
 310 estimate. However, if they are not linearly additive then there may be an imprint on
 311 the attributable warming estimate, meaning that it will not be appropriate to apply a
 312 temporal filter. Figure 3 shows the difference in attributable ocean warming estimates for
 313 January 1992 (soon after the major eruption of Mt. Pinatubo) and for January 1997 (a
 314 while after, with no major eruptions occurring in the interim). No temporal smoothing
 315 was used for this map. The magnitude of the differences is comparable to those seen
 316 in the left panel of Figure 2, which is also a comparison of estimates with no temporal
 317 smoothing between Januaries five years apart but during an eruptionless period. More
 318 systematically, the root-mean-squared differences between the spatial patterns of estimated
 319 attributable warming over the ocean for each calendar month (not shown) do not indicate
 320 anything special about the years during and following the major Mt. Agung, El Chichón,
 321 or Mt. Pinatubo eruptions. We therefore adopt the 5-year boxcar smoothing in all further
 322 calculations.

323 4.6 Amplitude of response

324 Is the estimated attributable warming plausible? We expect the Nat-Hist/CMIP5-est1
 325 SSTs to have a near-zero trend, because the historicalNat simulations on which the Nat-
 326 Hist/CMIP5-est1 attributable warming calculation is predicated have a near-zero trend
 327 on multi-decadal time-scales. The 1961-2015 trends in the All-Hist SSTs based on the
 328 Hurrell et al. (2008) and NOAA OI.v2 observed products are shown in Figure 4 along
 329 with the Nat-Hist/CMIP5-est1 SSTs calculated by subtracting the Nat-Hist/CMIP5-est1
 330 attributable warming signal from the observed All-Hist SSTs. While there is little long-
 331 term trend over the Indian, South Pacific, and North Atlantic Oceans, sizeable areas of
 332 the North Pacific, South Atlantic, and Antarctic Oceans have cooling trends in the Nat-
 333 Hist/CMIP5-est1 SSTs that rival the magnitude of some of the warming trends in the
 334 All-Hist observations. The Antarctic cooling results from the observed cooling magnified
 335 by subtraction of a non-zero attributable warming signal in the CMIP5 data; it may be
 336 relevant that observational monitoring is quite poor in this area (better since 1982 with
 337 satellite monitoring). The North Pacific does not warm as much as other basins in the

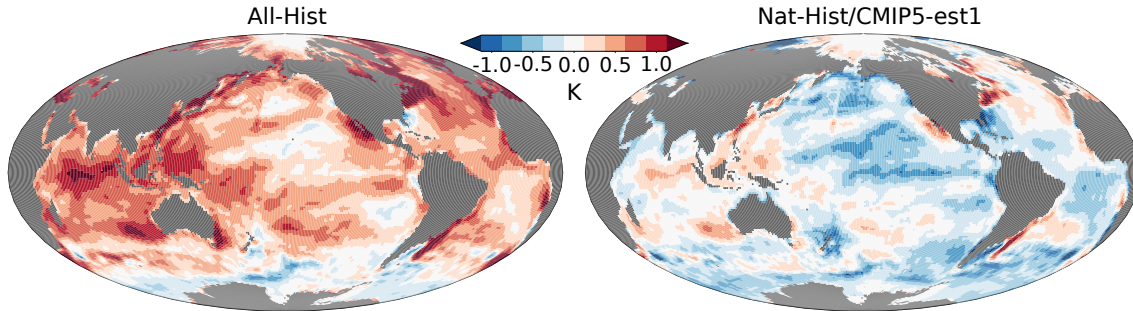


Figure 4: Map of 1961-2015 trends in All-Hist ocean temperatures, as recorded in Hurrell et al. (2008) and NOAA OI.v2 (left), and in Nat-Hist/CMIP5-est1 sea surface temperatures calculated by subtracting the Nat-Hist/CMIP5-est1 attributable warming estimate from the Hurrell et al. (2008) and NOAA OI.v2 data (right). Note that the Hurrell et al. (2008) product adopts NOAA OI.v2 in later decades, so here we have simply extended Hurrell et al. (2008) with the regular NOAA OI.v2 updates.

338 All-Hist map, possibly due to aliasing with the Pacific Decadal Oscillation which has gone
 339 from the negative to the positive to the negative phase during this period.

340 Overall, there is a 0.15°C cooling over the 50°S – 50°N ocean surface (a 0.17°C cooling
 341 including all latitudes) during the 1961–2015 period in the Nat-Hist/CMIP5-est1 SSTs
 342 when it is based on the Hurrell et al. (2008)/NOAA OI.v2 observational sea surface tem-
 343 perature product, compared to a 0.51°C All-Hist warming with that product (0.45°C
 344 warming including all latitudes). If instead the HadISST1 observed SST product (Rayner
 345 et al. 2003) is used, then the Nat-Hist/CMIP5 SSTs cool by 0.18°C compared to a 0.48°
 346 warming of the observed All-Hist ocean over 50°S – 50°N , or 0.19°C cooling compared to
 347 0.43°C warming globally. In comparison, the CMIP5 historical and historicalNat simula-
 348 tions warm (in skin temperature) by 0.66°C and 0.08°C respectively over the 50°S – 50°N
 349 ocean during 1961-2010 (the value for All-Hist and Nat-Hist/CMIP5-est1 SSTs over that
 350 period is a 0.45°C warming and a 0.13°C cooling respectively).

351 We can also evaluate the magnitude of the response through regression against the
 352 observed record. We take the global mean and annual mean skin temperatures over ocean
 353 areas averaged across all of the historical&rcp45 CMIP5 simulations listed in Table 2
 354 ($T(\bar{x}, \bar{m}, a, \bar{s}, \text{historical}\&\text{rcp45})$), do the same for the historicalNat simulations ($T(\bar{x}, \bar{m}, a, \bar{s}, \text{historicalNat})$),
 355 and take the global mean from the Hurrell et al. (2008) observational (All-Hist) product
 356 of sea surface temperatures ($SST(\bar{x}, \bar{m}, a, 0, \text{All-Hist})$, where the “0” denotes the single
 357 realisation). We then regress 5-year-averages ($a_{5\text{year}}$) of these historical&rcp45 and his-
 358 toricalNat signals using the total least squares regression approach (Allen and Stott 2003,
 359 v3.1.2 code at http://climate.web.runbox.net/detect_lib/). If β represents a regression
 360 coefficient and $\epsilon(a_{5\text{year}})$ represents the residual in the regression, then

$$\begin{aligned}
 SST(\bar{x}, \bar{m}, a_{5\text{year}}, 0, \text{All-Hist}) & \\
 &= \beta_{\text{historical}\&\text{rcp45}} (T(\bar{x}, \bar{m}, a_{5\text{year}}, \bar{s}, \text{historical}\&\text{rcp45}) - \epsilon_{\text{historical}\&\text{rcp45}}(a_{5\text{year}})) \\
 &+ \beta_{\text{historicalNat}} (T(\bar{x}, \bar{m}, a, \bar{s}, \text{historicalNat}) - \epsilon_{\text{historicalNat}}(a_{5\text{year}})) + \epsilon_{\text{observed}}(a_{5\text{year}}).
 \end{aligned} \tag{1}$$

361 The residual is compared against available skin temperature data from unforced (i.e. no
 362 changes in external boundary conditions beyond the diurnal and annual cycles) “piCon-
 363 trol” simulations from all of the CMIP5 models listed in Table 2 (except no data is available

Table 3: 90% confidence ranges on regression coefficients from 2-way regression of the CMIP5 historical&rcp45 and historicalNat climate model output against the Hurrell et al. (2008) observed sea surface temperature record. Values marked with asterisks fail the goodness-of-fit test on the residuals. The confidence ranges and goodness-of-fit are estimated with unforced simulations providing 79 samples for 110-year trends and 175 for 50-year trends.

Period	Domain	Annual	January	April	July	October
1901–2010	Ocean, global	0.87,1.16*	0.83,1.12*	0.87,1.18*	0.88,1.19*	0.87,1.15*
1901–2010	Ocean, 50°S–50°N	0.91,1.19*	0.87,1.16*	0.90,1.20*	0.91,1.20*	0.91,1.18*
1961–2010	Ocean, global	0.58,1.02	0.47,0.96	0.62,1.08	0.64,1.09	0.55,0.99
1961–2010	Ocean, 50°S–50°N	0.62,1.05	0.54,0.99	0.65,1.09	0.65,1.09	0.60,1.03

364 for BCC-CSM-1). The 90% confidence range on the regression coefficient for the response
365 to anthropogenic forcing is listed in Table 3 for a number of periods, domains, and months
366 of the year. No years past 2010 are considered in these regressions due to availability of
367 CMIP5 climate model output.

368 For the century-long time scale, the most likely estimates for the regression coefficients
369 are near 1, meaning that the magnitude of the long-term change in the Nat-Hist/CMIP5-
370 est1 attributable warming estimate is consistent with the magnitude of the observed trends.
371 However, the residual of the regression is significantly larger than would be expected
372 with an adequate fit. This inconsistency results from a warm bias in the CMIP5 histor-
373 ical&rcp45 simulations relative to observed values at the beginning of the 20th Century
374 and a relative cold bias in the middle of the century, which can be at least partially re-
375 duced by considering the responses to greenhouse gas forcing and anthropogenic aerosols
376 forcing separately, i.e. through a regression analysis that isolates these responses (Ribes
377 and Terray 2013).

378 A more relevant analysis, however, would examine the 1961–2010 period, both because
379 the observational monitoring is more comprehensive for this period and because it more
380 closely matches with periods likely to be examined in the C20C+ D&A Project and similar
381 investigations. Because the temporal profile of the aerosol and greenhouse gas responses is
382 similar (but opposite) over the past half century, a regression analysis distinguishing only
383 anthropogenic and natural signals over the past half-century is able to produce an adequate
384 fit to the observed record over this period, but at the cost of regression coefficients that
385 are barely consistent with 1 (Table 3). Thus, it may be possible to improve the accuracy
386 of the Nat-Hist/CMIP5-est1 attributable warming estimate through adjustments based
387 on a multi-signal regression analysis such as is performed in this test. However, we note
388 that recent progress in data recovery and analysis have tended to increase estimates of the
389 observed rate of warming in comparison to the ocean temperature products considered
390 above (Karl et al. 2015). Also, sea surface temperatures in the past few years have been
391 markedly higher than during the decade ending in 2010 (the last decade used for the
392 regression analysis performed here), suggesting that the existence of the discrepancy may
393 be sensitive to the choice of period. In light of this uncertainty, the Nat-Hist/CMIP5-est1
394 attributable warming estimate appears to have an acceptable possible warm bias and that
395 the added complexity of a regression-based adjustment is not required.

396 5 Sea ice coverage

397 Unfortunately, the attributable change in sea ice coverage cannot be diagnosed in the same
398 manner as the attributable ocean warming. Regional biases in sea ice extent in the CMIP5
399 models (Mahlstein et al. 2013; Flato et al. 2013; Notz 2014), as well as inconsistencies in
400 subtracting a mean difference from a temporally-varying observed extent, lead to implausi-
401 ble Nat-Hist estimates. Recognising this, Pall et al. (2011) instead developed an approach
402 to alter sea ice coverage in a manner that is consistent with the estimated Nat-Hist SSTs.
403 This method involves determining a simple functional form to the SST–SIC relationship
404 and modifying the All-Hist ice coverage using this function. Pall et al. (2011) adopted a
405 function that depends on a linear fit passing through the freezing-point/full-coverage point
406 and the median temperature/coverage point of all intermediate-coverage areas as deter-
407 mined from observed grid-cell-resolution data, the function being estimated separately for
408 each hemisphere. The function then followed three basic steps (see inset Figure 5):

- 409 • If the Nat-Hist temperature is below the freezing point, enforce full coverage.
- 410 • While at temperatures above the intercept of the linear fit and no-coverage, maintain
411 the All-Hist coverage.
- 412 • While the temperature is between the freezing point and the intercept of the linear
413 fit and no-coverage, increase the coverage at the rate indicated by the linear fit.

414 The approach has been used by a number of recent studies (Christidis et al. 2013; Sh-
415 iogama et al. 2013; Christidis and Stott 2014), but its performance has yet to be examined
416 in detail. We adopt a similar function here except that the intermediate-coverage section
417 is estimated using a bin-based approach, as a check to confirm an approximately linear re-
418 lationship. We calculate the median temperature in each of 100 equally-sized ice-coverage
419 bins, and the new function is the line that connects the freezing-point/full-coverage point
420 and the centre of mass of all of the bin medians. The calculations are performed on ob-
421 served temperature/ice-coverage data over the 2001-2010 period using the NOAA OI.v2
422 observationally-based dataset (Reynolds et al. 2002). The result ends up being similar
423 to the linear fit of Pall et al. (2011) (dashed red versus dashed blue lines in the plots
424 in the top two rows of Figure 6). This bin-based empirical fit has a slope of $\phi(x)$ and
425 a no-coverage intercept at $SST_{open}(x)$, and is estimated and applied separately for the
426 Northern and Southern Hemispheres (denoted via dependence on location x).

427 Given this function, the algorithm for determining the Nat-Hist ice coverage follows a
428 series of steps, listed in Figure 5. The resulting changes are illustrated in Figure 6, when
429 the Nat-Hist/CMIP5-est1 attributable warming estimate is applied to the NOAA OI.v2
430 observational product. The profile of the centre-of-mass of the bins (solid red lines in the
431 top and middle left panels of Figure 6) is nearly linear, the linear fit (dotted red line) is
432 very close to the linear fit used by Pall et al. (2011). Because of the way the function
433 starts increasing ice coverage deterministically at $SST_{open}(x)$, the visual difference between
434 the SST–SIC scatter before (top and middle left panels) and after (top and middle central
435 panels) is a thinning of the scatter at low SIC values. A notable issue is that the function is
436 limited in its ability to handle attributable cooling (i.e. sea ice retreat due to the Nat-Hist
437 conditions being warmer than the observed/All-Hist conditions). In particular, because
438 available observational products fix surface temperature to the freezing point when ice
439 coverage is full, it is not possible to thin the full-coverage ice in a sensible way following
440 this sort of method. One solution would be to use skin temperature, but the required
441 multi-decadal observations are lacking. Fortunately, for the intended application here this
442 issue is not relevant because no regions near sea ice exhibit an attributable cooling.

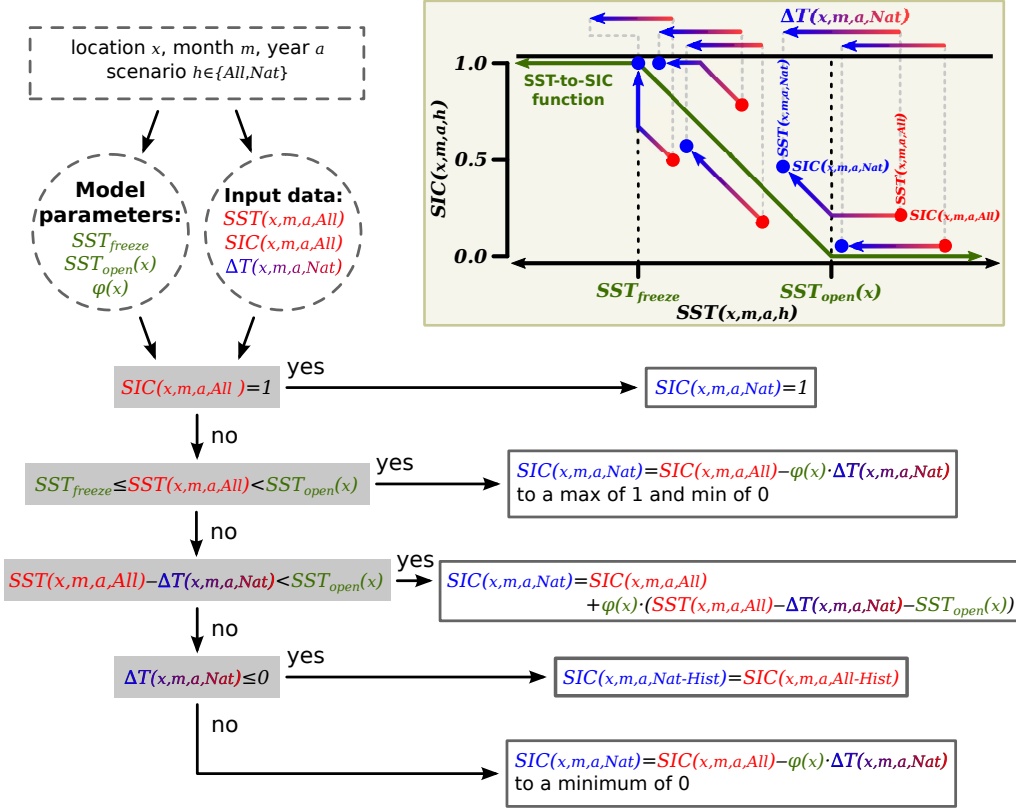


Figure 5: The algorithm used for estimating counterfactual Nat-Hist fractional sea ice coverage, $SIC(x, m, a, 0, Nat-Hist)$, in a cell x on the target spatial grid during month m of year a . The inputs are the factual All-Hist (observed) sea surface temperature, $SST(x, m, a, 0, All-Hist)$, and fractional sea ice coverage, $SIC(x, m, a, 0, All-Hist)$, along with the attributable warming estimate for the location, $\Delta T(x, m, a, \bar{s}, Nat-Hist/CMIP5-est1)$. The inset shows example cases schematically. The s variable and “-Hist” in the All-Hist and Nat-Hist variable values have been omitted in the figure for conciseness. SST_{freeze} is the freezing temperature of sea water (-1.8°C in the NOAA OI.v2 observationally-based data product). See text for further details.

443 While the results in Figure 6 look plausible, we can evaluate the method more directly
 444 by using it to estimate All-Hist sea ice coverage from observed sea surface temperatures,
 445 and then comparing against the actual observed sea ice coverage. Usage of the algorithm
 446 as an actual predictor, rather than a delta on existing values, should be a strong test. To
 447 do this, the sea ice coverage is defined:

- 448 • As full when $SST(x, m, a, 0, All-Hist) = SST_{freeze}$
 449 (note $SST(x, m, a, 0, All-Hist) \geq SST_{freeze}$);
- 450 • As $\phi(x) \cdot (SST(x, m, a, 0, All-Hist) - SST_{open}(x))$
 451 when $SST_{freeze} < SST(x, m, a, 0, All-Hist) < SST_{open}(x)$;
- 452 • As zero when $SST_{open}(x) < SST(x, m, a, 0, All-Hist)$.

453 Results are shown in Figure 7. The estimated values tend to lag in both the spring
 454 and autumn, reflecting a lack of a consideration of freezing or melting physics in the
 455 algorithm. Coverage also tends to be overestimated in the Arctic during the winter by

456 about 1 million km². As seen in the maps, there can be some regional differences which
457 could be relevant for the generation of extreme weather over nearby land. However,
458 considering the algorithm is intended only for estimating perturbations from observed
459 conditions, this usage as a direct predictor should be considered an indication of what the
460 maximum possible errors can be, rather than what they are likely to be in regular usage.

461 Does the method produce expected near-zero trends in Nat-Hist/CMIP5-est1 sea
462 ice coverage? Figure 8 shows the trends over the 1961-2015 in the All-Hist and Nat-
463 Hist/CMIP5-est1 sea ice concentration when using the Hurrell et al. (2008) and NOAA OI.v2
464 products. In the Northern Hemisphere, the Nat-Hist/CMIP5-est1 SICs increase north of
465 Norway and adjacent to the Kamchatka Peninsula and the Kuril Islands at a rate compa-
466 rable to the fastest retreat seen in the All-Hist SICs. In other regions there is little change
467 in the Nat-Hist/CMIP5-est1 SICs, so overall the Northern Hemisphere Nat-Hist/CMIP5-
468 est1 advance is about half the size of the All-Hist retreat. Over the Southern Hemisphere,
469 however, there is a widespread advance of Nat-Hist/CMIP5-est1 SICs, in comparison to
470 little trend in the All-Hist SICs. It is difficult to be sure about the accuracy of the ob-
471 served SICs around Antarctica before 1982 on which these trend calculations are based,
472 but needless to say such a large Nat-Hist/CMIP5-est1 advance is not what would be ex-
473 pected under the absence of anthropogenic forcing. This Southern Hemisphere result is
474 entirely consistent with the anthropogenic ocean warming around Antarctica in the CMIP5
475 historical&rcp45 simulations and the lack of warming in observational products. As such
476 it does not really serve as a test of the sea ice algorithm used here, but rather as a flag on
477 a regional warming in the CMIP5 historical&rcp45 simulations that is not supported by
478 the observational record.

479 6 Discussion

480 This paper has described the development of an estimate of the ocean warming and associ-
481 ated sea ice retreat attributable to anthropogenic emissions, for use in generating a scenario
482 (dubbed Nat-Hist/CMIP5-est1) of what the ocean surface might have been in the absence
483 of those emissions. This estimate is based on the difference in multi-model-mean skin tem-
484 peratures of simulations available in the CMIP5 database, between simulations forced with
485 historical anthropogenic and natural drivers versus simulations forced by natural drivers
486 only. In Section 3 we proposed four criteria for a benchmark estimate: physical plausibil-
487 ity, robustness, obviousness, and availability. Here we evaluate the Nat-Hist/CMIP5-est1
488 SSTs and SICs against these criteria.

489 Considering the nature of the underlying source of data, the Nat-Hist/CMIP5-est1 at-
490 tributable warming and resulting SSTs and SICs are physically plausible. The underlying
491 climate models are explicitly constructed to simulate the interactions and evolution of the
492 various physical components of the climate system. Comparisons against the observational
493 record suggest that the Nat-Hist/CMIP5-est1 attributable warming estimate may over-
494 estimate the global amplitude of the warming attributable to anthropogenic emissions.
495 In general the regional Nat-Hist/CMIP5-est1 SSTs appear plausible, but the long-term
496 trends in Nat-Hist/CMIP5-est1 SICs flag some regions, particularly near the sea ice edge,
497 where the attributable warming estimate is not specifically supported by the observational
498 record. This is the most significant possible weakness identified here.

499 The Nat-Hist/CMIP5-est1 attributable warming estimate and resulting SSTs and SICs
500 are robust against perturbations to data selection, possible nonlinearities due to the oc-
501 currence of volcanic eruptions, and choice of year. We argue that the data source, possibly
502 the most used in the world for detection and attribution purposes, and historical-minus-

503 historicalNat-based method are common enough to satisfy the obviousness criterion. Es-
504 timates based on a single atmosphere-ocean climate model suffer from the issue that the
505 method of selecting the model is not universally obvious, and results appear to be sen-
506 sitive to that issue; in contrast the Nat-Hist/CMIP5-est1 attributable warming estimate
507 appears robust against the exact method of selecting simulations from available climate
508 models because of the large pool of simulations and models used (Section 4.4).

509 In terms of availability, the data products used consist of easily accessible observational
510 products and CMIP5 output, and the methodology is simple enough that it should be
511 straightforward to reproduce. Moreover, the Nat-Hist/CMIP5-est1 attributable warming
512 estimate, as well as the Nat-Hist/CMIP5-est1 SSTs and SICs resulting from application to
513 both the combined Hurrell et al. (2008) and NOAA OI.v2 (labeled as NOAA OI.v2) obser-
514 vational product and the HadISST1 observational product are freely downloadable online
515 at <http://portal.neresc.gov/c20c/data/C20C/> as part of the C20C+ D&A project, as is the
516 code for their generation at <http://portal.neresc.gov/c20c/experiment.html#TOOLS>.

517 Some recent studies have conducted factual real-world versus counterfactual natural-
518 world experiments under a weather hindcast setup (Takayabu et al. 2015; Pall et al. 2017;
519 Wehner et al. 2019). In these experiments, a standard ensemble hindcast is compared
520 against a modified hindcast in which SSTs, initial boundary conditions, and lateral bound-
521 ary conditions for a regional downscaling model are modified through subtraction of an at-
522 tributable anthropogenic component. Using the same method and CMIP5 models described
523 above for the Nat-Hist/CMIP5-est1 attributable SST warming, we have calculated consis-
524 tent Nat-Hist/CMIP5-est1 attributable sea level pressure change and attributable three-
525 dimensional change in atmospheric geopotential height, temperature, specific humidity,
526 zonal wind, and meridional wind (available at <http://portal.neresc.gov/c20c/data/C20C/>).
527 With this set of attributable changes, it will be possible to compare and contrast the hind-
528 cast approach with the free-running global climate model approach, under a controlled
529 experiment design.

530 However, this estimate is by no means the only possible one, and even if it is adopted
531 as a benchmark it should not be used exclusively. In addition to existing estimates de-
532 scribed in Section 3, here we briefly mention other possible estimates related to this Nat-
533 Hist/CMIP5-est1 estimate:

534 **Sampling of amplitude uncertainty:** If we assume separability of the attributable
535 warming pattern and the amplitude of that pattern, the regression analysis described
536 in Section 4.6 can also calculate the probability distribution of values for the regres-
537 sion coefficient informed by observed trends. Usage of the same pattern but different
538 amplitudes corresponding to specified quantiles of this probability distribution can
539 yield markedly different estimates of the magnitude of the role of anthropogenic
540 emissions in the chance of extreme weather (Pall et al. 2011).

541 **Sampling individual atmosphere-ocean climate models :** One possible criticism of
542 the attributable warming estimate used for the Nat-Hist/CMIP5-est1 scenario is that
543 it is not necessarily physically consistent, i.e. in a nonlinear climate system averaging
544 across models may produce changes in circulation that are not physically plausible.
545 This issue would be remedied by selecting simulations from just a single climate
546 model. Indeed, the few studies that have used more than one such estimate have
547 found major differences in results, highlighting the importance of examining mul-
548 tiple estimates (Pall et al. 2011; Kay et al. 2011; Christidis et al. 2012; Shiogama
549 et al. 2014; Christidis and Stott 2014; Schaller et al. 2016). The 5-year temporal
550 filter could be expanded to deal with the smaller sample size of simulations (Sh-

551 iogama et al. 2013, Section 4.5), but not too much; spatial smoothing is another
552 option (Shiogama et al. 2013) but it would remove much of the small-scale fea-
553 tures that are vital aspects of the differences between single-model estimates. Thus,
554 single-model estimates would likely retain a substantial amount of sampling noise.
555 Following the above methods (but using an 11-year temporal filter), a number of
556 single-model attributable warming estimates have been calculated and are provided
557 at <http://portal.nersc.gov/c20c/data/C20C/>.

558 **Usage of a different sea ice coverage estimator:** Differences in treatment of how sea
559 ice coverage should be altered may be important for attribution studies at high lat-
560 itudes (Angélil et al. 2014). Permutations on the method developed here, including
561 seasonally-varying ϕ and SST_{open} parameters for the SST-SIC function, are one op-
562 tion. Otto et al. (2015) used a different method following from the development
563 of the HadISST1 product, but it has substantial biases when applied to other ob-
564 servational products (J. Imbers, pers. comm.). A method that can yield plausible
565 sea ice retreat would, however, be useful for examining a counterfactual world with-
566 out aerosol emissions (but with historical greenhouse gas emissions), for instance.
567 Overall, though, the tests conducted above suggest that biases in attributable SST
568 warming may be the biggest source of error in natural-world SIC estimates.

569 Beyond the variations described above, other possibilities could be more observa-
570 tionally focussed (Christidis and Stott 2014), for instance using pattern scaling methods
571 (Bichet et al. 2015; 2016). Ultimately, it is hoped that both hardware and software will
572 develop to the point where large-ensemble, high-spatial-resolution experiments are possi-
573 ble with fully coupled atmosphere-ocean-land-ice models, at which point offline estimation
574 of the attributable ocean warming and sea ice retreat will become obsolete.

575 Acknowledgements

576 This material is based upon work supported by the U.S. Department of Energy, Office
577 of Science, Office of Biological and Environmental Research, under contract number DE-
578 AC02-05CH11231, and by the New Zealand Ministry of Business, Innovation and Employ-
579 ment. This work was gratefully assisted by discussions with Myles Allen, Nikos Christidis,
580 Marty Hoerling, Jara Imbers Quintana, Judith Perlwitz, Cameron Rye, Hideo Shiogama,
581 Peter Stott, Simon Tett, and Michael Wehner, as well as the Attribution of Climate-related
582 Events activity. The National Energy Research Scientific Computing Center, a DOE Of-
583 fice of Science User Facility supported by the Office of Science of the U.S. Department
584 of Energy under Contract No. DE-AC02-05CH11231, hosts the C20C+ D&A project
585 portal from which the data sets described in this paper can be obtained. The authors
586 also acknowledge the World Climate Research Programme’s Working Group on Coupled
587 Modelling, which is responsible for CMIP, and thank the climate modeling groups (listed
588 in Table 2) for producing and making available their model output. For CMIP the U.S.
589 Department of Energy’s Program for Climate Model Diagnosis and Intercomparison pro-
590 vides coordinating support and led development of software infrastructure in partnership
591 with the Global Organization for Earth System Science Portals. NOAA’s Environmental
592 Modeling Center, the Community Earth System Model project, and the U.K. Met Office
593 are acknowledged for the NOAA OI.v2, Hurrell et al. (2008), and HadISST1 products
594 respectively.

595 **References**

- 596 Allen, M. R. and P. A. Stott, 2003: Estimating signal amplitudes in optical fingerprinting,
597 part I: theory. *Clim. Dyn.*, **21**, 477–491.
- 598 Angélic, O., D. A. Stone, M. Tadross, F. Tummon, M. Wehner, and R. Knutti, 2014:
599 Attribution of extreme weather to anthropogenic greenhouse gas emissions: sensitivity
600 to spatial and temporal scales. *Geophys. Res. Lett.*, **41**, 2150–2155.
- 601 Bichet, A., P. J. Kushner, and L. Mudryk, 2016: Estimating the continental response to
602 global warming using pattern-scaled sea surface temperatures and sea ice. *J. Climate*,
603 **29**, 9125–9139.
- 604 Bichet, A., P. J. Kushner, L. Mudryk, L. Terray, and J. C. Fyfe, 2015: Estimating the
605 anthropogenic sea surface temperature response using pattern scaling. *J. Climate*, **28**,
606 3751–3763.
- 607 Bindoff, N. L., P. A. Stott, K. M. AchutaRao, M. R. Allen, N. Gillett, D. Gutzler,
608 K. Hansingo, G. Hegerl, Y. Hu, S. Jain, I. I. Mokhov, J. Overland, J. Perlwitz, R. Seb-
609 bari, X. Zhang, and et alii, 2013: Detection and attribution of climate change: from
610 global to regional, *Climate Change 2013: The Physical Science Basis. Contribution*
611 *of Working Group I to the Fifth Assessment Report of the Intergovernmental Panel*
612 *on Climate Change*, T. F. Stocker, D. Qin, G.-K. Plattner, M. Tignor, S. K. Allen,
613 J. Boschung, A. Nauels, Y. Xia, V. Bex, and P. M. Midgley, eds., Cambridge University
614 Press, 867–952.
- 615 Christidis, N. and P. A. Stott, 2014: Change in the odds of warm years and seasons due
616 to anthropogenic influence on the climate. *J. Climate*, **27**, 2607–2621.
- 617 Christidis, N., P. A. Stott, A. A. Scaife, A. Arribas, G. S. Jones, D. Copey, J. R. Knight,
618 and W. J. Tennant, 2013: A new HadGEM3-A-based system for attribution of weather-
619 and climate-related extreme events. *J. Climate*, **26**, 2756–2783.
- 620 Christidis, N., P. A. Stott, F. W. Zwiers, H. Shiogama, and T. Nozawa, 2012: The con-
621 tribution of anthropogenic forcings to regional changes in temperature during the last
622 decade. *Clim. Dyn.*, **39**, 1259–1274.
- 623 Deser, C., A. S. Phillips, and M. A. Alexander, 2010: Twentieth century tropical sea
624 surface temperature trends revisited. *Geophys. Res. Lett.*, **37**.
- 625 Dong, B., R. T. Sutton, L. Shaffrey, and N. P. Klingaman, 2017: Attribution of forced
626 decadal climate change in coupled and uncoupled ocean-atmosphere model experiments.
627 *J. Climate*.
- 628 Flato, G., J. Marotzke, B. Abiodun, P. Braconnot, S. C. Chou, W. Collins, P. Cox, F. Dri-
629 ouech, S. Emori, V. Eyring, C. Forest, P. Gleckler, E. Guilyardi, C. Jakob, V. Kattsov,
630 C. Reason, M. Rummukainen, and et alii, 2013: Evaluation of climate models, *Climate*
631 *Change 2013: The Physical Science Basis. Contribution of Working Group I to the Fifth*
632 *Assessment Report of the Intergovernmental Panel on Climate Change*, T. F. Stocker,
633 D. Qin, G.-K. Plattner, M. Tignor, S. K. Allen, J. Boschung, A. Nauels, Y. Xia, V. Bex,
634 and P. M. Midgley, eds., Cambridge University Press, 741–866.

- 635 Gillett, N. P., H. Shiogama, B. Funke, G. Hegerl, R. Knutti, K. Matthes, B. D. Santer,
636 D. Stone, and C. Tebaldi, 2016: The Detection and Attribution Model Intercomparison
637 Project (DAMIP v1.0) contribution to CMIP6. *Geosci. Model Dev.*, **9**, 3685–3697.
- 638 Gillett, N. P., M. F. Wehner, S. F. B. Tett, and A. J. Weaver, 2004: Testing the linearity
639 of the reponse to combined greenhouse gas and sulfate aerosol forcing. *Geophys. Res.
640 Lett.*, **31**.
- 641 Hartmann, D. L., A. M. G. Klein Tank, M. Rusticucci, L. V. Alexander, S. Brönnimann,
642 Y. Charabi, F. J. Dentener, E. J. Dlugokencky, D. R. Easterling, A. Kaplan, B. J.
643 Soden, P. W. Thorne, M. Wild, P. Zhai, and et alii, 2013: Observations: atmosphere and
644 surface, *Climate Change 2013: The Physical Science Basis. Contribution of Working
645 Group I to the Fifth Assessment Report of the Intergovernmental Panel on Climate
646 Change*, T. F. Stocker, D. Qin, G.-K. Plattner, M. Tignor, S. K. Allen, J. Boschung,
647 A. Nauels, Y. Xia, V. Bex, and P. M. Midgley, eds., Cambridge University Press, 159–
648 254.
- 649 Hegerl, G. C., F. W. Zwiers, P. Braconnot, N. P. Gillett, Y. Luo, J. A. Marengo Orsini,
650 N. Nicholls, J. E. Penner, P. A. Stott, and et alii, 2007: Understanding and attributing
651 climate change, *Climate Change 2007: The Physical Science Basis. Contribution of
652 Working Group I to the Fourth Assessment Report of the Intergovernmental Panel on
653 Climate Change*, S. Solomon, D. Qin, M. Manning, Z. Chen, M. Marquis, K. B. Averyt,
654 M. Tignor, and H. L. Miller, eds., Cambridge University Press, Cambridge, U.K., 663–
655 745.
- 656 Herring, S. C., N. Christidis, A. Hoell, M. P. Hoerling, and P. A. Stone, 2018: Explaining
657 extreme events of 2017 from a climate perspective. *Bull. Amer. Meteor. Soc.*, **100**,
658 S1–S117.
- 659 Hoegh-Guldberg, O., R. Cai, E. s. Poloczanska, P. G. Brewer, S. Sundby, K. Hilmi, V. J.
660 Fabry, S. Jung, and et alii, 2014: The Ocean, *Climate Change 2014: Impacts, Adapta-
661 tion, and Vulnerability. Part B: Regional Aspects. Contribution of Working Group II to
662 the Fifth Assessment Report of the Intergovernmental Panel on Climate Change*, V. R.
663 Barros, C. B. Field, and et alii, eds., Cambridge University Press, 1655–1731.
- 664 Hurrell, J. W., J. J. Hack, D. Shea, J. M. Caron, and J. Rosinski, 2008: A new sea surface
665 temperature and sea ice boundary dataset for the Community Atmosphere Model. *J.
666 Climate*, **21**, 5145–5153.
- 667 Karl, T. R., A. Arguez, B. Huang, J. H. Lawrimore, J. R. McMahon, M. J. Menne, T. C.
668 Peterson, R. S. Vose, and H.-M. Zhang, 2015: Possible artifacts of data biases in the
669 recent global surface warming hiatus. *Science*, **348**, 1469–1472.
- 670 Kay, A. L., S. M. Crooks, P. Pall, and D. A. Stone, 2011: Attribution of Autumn/Winter
671 2000 flood risk in England to anthropogenic climate change: a catchment-based study.
672 *J. Hydrol.*, **406**, 97–112.
- 673 Kennedy, J. J., 2014: A review of uncertainty in in situ measurements and data sets of
674 sea surface temperature. *Rev. Geophys.*, **52**, 1–32.
- 675 Mahlstein, I., P. R. Gent, and S. Solomon, 2013: Historical Antarctic mean sea ice area,
676 sea ice trends, and winds in CMIP5 simulations. *J. Geophys. Res.*, **118**, 5105–5110,
677 10.1002/jgrd.50443.

- 678 Meehl, G. A., W. M. Washington, T. M. L. Wigley, J. M. Arblaster, and A. Dai, 2003:
679 Solar and greenhouse gas forcing and climate response in the twentieth century. *J.*
680 *Climate*, **16**, 426–444.
- 681 National Academies of Sciences, Engineering, and Medicine, 2016: *Attribution of extreme*
682 *weather events in the context of climate change*, The National Academies Press.
- 683 Notz, D., 2014: Sea-ice extent and its trend provide limited metrics of model performance.
684 *Cryosphere*, **8**, 229–243.
- 685 Otto, F. E. L., S. M. Rosier, M. R. Allen, N. R. Massey, C. J. Rye, and J. Imbers Quintana,
686 2015: Attribution analysis of high precipitation event in summer in England and Wales
687 over the last decade. *Clim. Change*, **132**, 77–91.
- 688 Pall, P., T. Aina, D. A. Stone, P. A. Stott, T. Nozawa, A. G. J. Hilberts, D. Lohmann, and
689 M. R. Allen, 2011: Anthropogenic greenhouse gas contribution to flood risk in England
690 and Wales in Autumn 2000. *Nature*, **470**, 382–385.
- 691 Pall, P., C. M. Patricola, M. F. Wehner, D. A. Stone, C. J. Paciorek, and W. D. Collins,
692 2017: Diagnosing anthropogenic contributions to heavy Colorado rainfall in September
693 2013. *Weather and Climate Extremes*, In press.
- 694 Rayner, N. A., D. E. Parker, E. B. Horton, C. K. Folland, L. V. Alexander, D. P. Rowell,
695 E. C. Kent, and A. Kaplan, 2003: Global analyses of sea surface temperature, sea ice,
696 and night marine air temperature since the late nineteenth century. *J. Geophys. Res.*,
697 **108**.
- 698 Reynolds, R. W., N. A. Rayner, T. M. Smith, D. C. Stokes, and W. C. Wang, 2002: An
699 improved in situ and satellite SST analysis for climate. *J. Clim.*, **15**, 1609–1625.
- 700 Ribes, A. and L. Terray, 2013: Application of regularised optimal fingerprinting to attribu-
701 tion. Part II: application to global near-surface temperature. *Clim. Dyn.*, **41**, 2837–2853.
- 702 Risser, M. D., D. A. Stone, C. J. Paciorek, M. F. Wehner, and O. Angélil, 2017: Quan-
703 tifying the effect of interannual ocean variability on the attribution of extreme climate
704 events to human influence. *Clim. Dyn.*.
- 705 Schaller, N., A. L. Kay, R. Lamb, N. R. Massey, G. J. van Oldenborgh, F. E. L. Otto,
706 S. N. Sparrow, R. Vautard, P. Yiou, I. Ashpole, A. Bowery, S. M. Crooks, K. Haustein,
707 C. Huntingford, W. J. Ingram, R. G. Jones, T. Legg, J. Miller, J. Skeggs, D. Wallom,
708 A. Weisheimer, S. Wilson, P. A. Stott, and M. R. Allen, 2016: Human influence on
709 climate in the 2014 southern England winter floods and their impacts. *Nature Clim.*
710 *Change*, **6**, 627–634.
- 711 Shiogama, H., D. A. Stone, T. Nagashima, T. Nozawa, and S. Emori, 2012: On the lin-
712 ear additivity of climate forcing-response relationships at global and continental scales.
713 *International Journal of Climatology*, **33**, 2542–2550.
- 714 Shiogama, H., M. Watanabe, Y. Imada, M. Mori, M. Ishii, and M. Kimoto, 2013: An
715 event attribution of the 2010 drought in the South Amazon region using the MIROC5
716 model. *Atmos. Sci. Lett.*, **14**, 170–175.
- 717 Shiogama, H., M. Watanabe, Y. Imada, M. Mori, Y. Kamae, M. Ishii, and M. Kimoto,
718 2014: Attribution of the June–July 2013 heat wave in the southwestern United States.
719 *SOLA*, **10**, 122–126.

- 720 Stone, D. A. and M. R. Allen, 2005: The end-to-end attribution problem: from emissions
721 to impacts. *Clim. Change*, **71**, 303–318.
- 722 Stone, D. A., N. Christidis, C. Folland, S. Perkins-Kirkpatrick, J. Perlwitz, H. Shiogama,
723 M. F. Wehner, P. Wolski, S. Cholia, H. Krishnan, D. Murray, O. Angéilil, U. Beyerle,
724 A. Ciavarella, A. Dittus, and X.-W. Quan, 2019: Experiment design of the interna-
725 tional clivar c20c+ detection and attribution project. *Weather and Climate Extremes*,
726 Submitted.
- 727 Stott, P. A., M. Allen, N. Christidis, R. Dole, M. Hoerling, C. Huntingford, P. Pall, J. Perl-
728 witz, and D. Stone, 2013: Attribution of weather and climate-related extreme events,
729 *Climate Science for Serving Society: Research, Modelling and Prediction Priorities*,
730 G. R. Asrar and J. W. Hurrell, eds., Springer, 307–337.
- 731 Sun, L., D. Allured, M. Hoerling, L. Smith, J. Perlwitz, D. Murray, and J. Eischeid, 2018:
732 Drivers of 2016 record Arctic warmth assessed using climate simulations subjected to
733 factual and counterfactual forcing. *Weather and Climate Extremes*, **19**, 1–9.
- 734 Takayabu, I., K. Hibino, H. Sasaki, H. Shiogama, N. Mori, Y. Shibutani, and T. Takemi,
735 2015: Climate change effects on the worst-case storm surge: a case study of Typhoon
736 Haiyan. *Environ. Res. Lett.*, **10**.
- 737 Taylor, K. E., R. J. Stouffer, and G. A. Meehl, 2012: An overview of CMIP5 and the
738 experiment design. *Bull. Amer. Met. Soc.*, **93**, 485–498.
- 739 Trenberth, K. E., J. T. Fasullo, and T. G. Shepherd, 2015: Attribution of climate extreme
740 events. *Nature Clim. Change*.
- 741 Wehner, M., Prabhat, K. A. Reed, D. Stone, W. D. Collins, and J. Bacmeister, 2015:
742 Resolution dependence of future tropical cyclone projections of CAM5.1 in the U.S.
743 CLIVAR Hurricane Working Group idealized configurations. *J. Clim.*, **28**, 3905–3925.
- 744 Wehner, M. F., Z. C., and C. Patricola, 2019: Estimating the human influence on tropical
745 cyclone intensity as the climate changes, *Hurricane Risk*, J. M. Collins and K. Walsh,
746 eds., Springer, 235–260.
- 747 Wehner, M. F., K. A. Reed, F. Li, Prabhat, J. T. Bacmeister, C. T. Chen, C. Paciorek,
748 P. J. Gleckler, K. R. Sperber, W. D. Collins, A. Gettelman, and C. Jablonowski, 2014:
749 The effect of horizontal resolution on simulation quality in the Community Atmospheric
750 Model, CAM5.1. *J. Adv. Model. Earth Syst.*, **6**, 980–997.
- 751 Wolski, P., D. Stone, M. Tadross, M. Wehner, and B. Hewitson, 2014: Attribution of
752 floods in the Okavango Basin, Southern Africa. *J. Hydrol.*, **511**, 350–358.

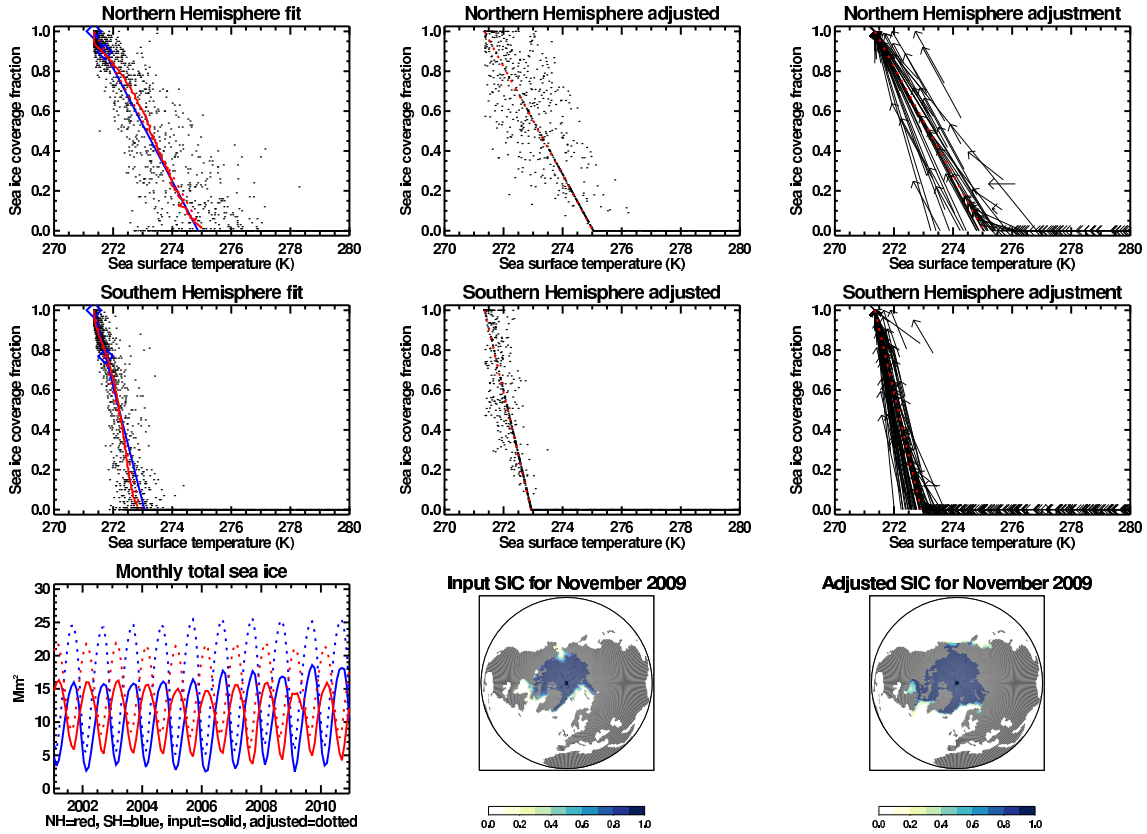


Figure 6: The estimation of attributable changes in sea ice coverage as implemented for the Nat-Hist/CMIP5-est1 scenario. The top two rows show data for the Northern Hemisphere (top row) and Southern Hemisphere (middle row). The left panels of these two rows show the sea ice coverage and sea surface temperature relationship during the 2001-2010 period in the NOAA OI.v2 observational product (Reynolds et al. 2002) (dots, only a limited number of points are displayed in order to avoid saturation), the Pall et al. (2011) linear fit for adjusting ice coverage (blue line, with the diamonds marking the points used to calculate the line), and the median temperature for each coverage bin (solid red line) and the resulting linear fit (dashed red line) used for the Nat-Hist/CMIP5-est1 scenario. The middle panels in the top two rows show the resulting temperature and coverage data estimates for the Nat-Hist/CMIP5-est1 scenario, while the right panels show the progression from observed values to Nat-Hist/CMIP5-est1 values. The bottom left panel shows the monthly coverage time series for both hemispheres (North in red, South in blue) as observed (solid) and under the Nat-Hist/CMIP5-est1, based on NOAA OI.v2. The two maps illustrate Arctic coverage for November 2009 from observed All-Hist (middle) and for the Nat-Hist/CMIP5-est1 scenario (right).

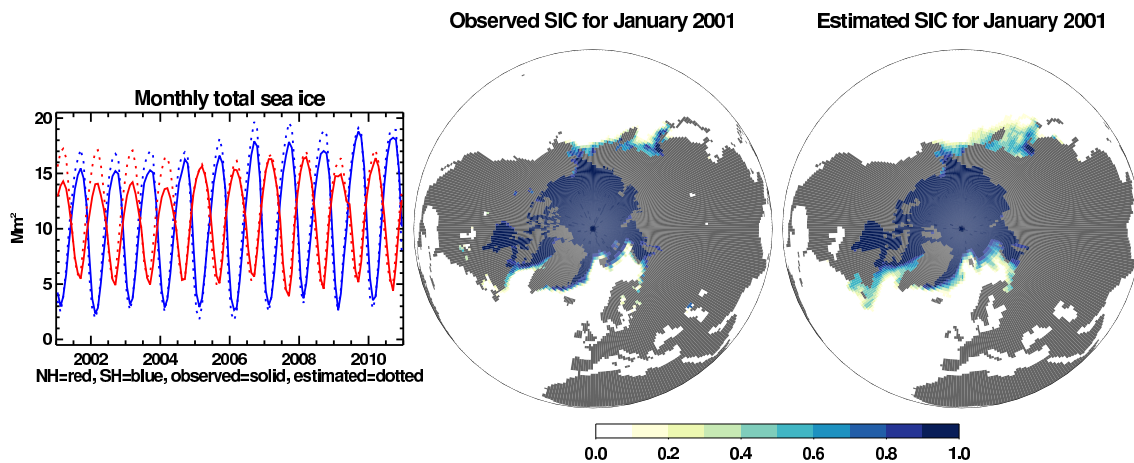


Figure 7: Comparison of sea ice coverage predicted directly from observed All-Hist sea surface temperatures using the algorithm described in Figure 5 versus observed All-Hist values. Left panel: Monthly mean values for the Northern (red) and Southern (blue) Hemispheres from the NOAA OI.v2 observational product (solid) and as estimated from the NOAA OI.v2 sea surface temperatures (dotted). Middle panel: Observed sea ice concentration according to NOAA OI.v2 for January 2001. Right panel: Predicted sea ice concentration based on NOAA OI.v2 sea surface temperatures.

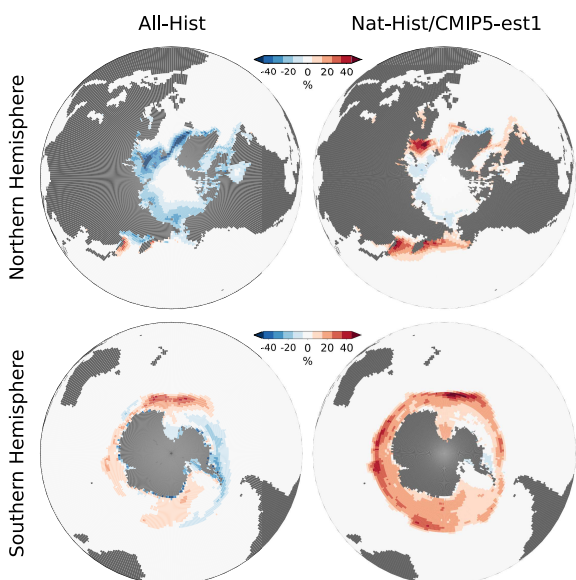


Figure 8: Map of 1961-2015 trends in All-Hist sea ice concentration, as recorded in Hurrell et al. (2008) (left), and in Nat-Hist/CMIP5-est1 sea ice concentration calculated from the Hurrell et al. (2008) and NOAA OI.v2 reference (right).